EVOLUTION OF NON-PERSISTENT WEAK LAYER AND SNOWPACK STABILITY DURING SNOWFALL

Hiroki Matsushita[1]*, Wataru Takahashi[1], Masaru Matsuzawa[1], and Joji Takahashi[1]

[1] *Civil Engineering Research Institute for Cold Region (CERI), Public Works Research Institute (PWRI), Sapporo, Japan*

ABSTRACT: To clarify the conditions under which avalanches triggered by the failure of the non-persistent weak layer are likely, field observations of temporal changes in the density and hardness of new snow layers consisting unrimed crystals (i.e., the non-persistent weak layer) and a theoretical examination related to the stability of snowpack on slope were carried out. The density and hardness increased more slowly in the non-persistent weak layer consisting of unrimed crystals than in the snow layer consisting of heavily rimed snow crystals. In addition, the snow consisting of unrimed crystals underwent rapid destabilization with less snowfall than the snow consisting of heavily rimed crystals did.

KEYWORDS: Non-persistent weak layer, Unrimed crystals, Snow density, Compressive viscosity.

1. INTRODUCTION

Dry-snow surface avalanches often are triggered when the non-persistent weak layers (McClung and Schaerer, 2006) consist of unrimed and/or lightly rimed crystals with broad branches (Akitaya and Shimizu, 1987; Bair, 2011; Ikeda, 2015). For evaluating the likelihood of dry-snow surface avalanches during snowfall, much research has been conducted: Empirical methods have used only snowfall amount (e.g., Bakkehϕi, 1986), theoretical (e.g., Endo, 1993; Conway and Wilbour, 1999; Matsushita and Ishida, 216) and statistical (e.g., Gauthier et al., 2010) methods have used meteorological data, and other methods have used physical-based numerical models to estimate the snowpack structure (e.g., Hirashima et al., 2008). However, these methods cannot evaluate the likelihood of an avalanche triggered by the failure of the non-persistent weak layer, and investigations on avalanche release resulting from such failure are insufficient. In particular, in order to evaluate the likelihood of avalanches associated with that layer during snowfall, it is necessary to understand temporal variations in the fracture toughness and density of the non-persistent weak layer (e.g., Brown and Jamieson, 2006, 2008; Ikeda, 2015).

In this paper, to clarify the conditions under which avalanches are likely to be triggered by the failure of the non-persistent weak layer, field observations of temporal changes in the hardness and density of new snow layers, observations of snow crystals, and a theoretical examination on the stability of snowpack on the slope were carried out.

* *Corresponding author address:*
Hiroki Matsushita, Civil Engineering Research Institute for Cold Region, Japan 062-8602;
tel: +81 11-841-1746; fax: +81 11-841-9747
email: matsushita-h@ceri.go.jp

2. METHODS

2.1 Field observation

The hardness and density of new snow layers were measured over time at Mt. Myoko (latitude: 36° 53' 50.75" N, longitude: 138° 9' 7.00" E, elevation (a.s.l.): 1067 m) in central Japan. We photographed newly fallen snow crystals and addressed the differences in temporal changes in hardnesses and densities between snow layers consisting of unrimed crystals and those consisting of heavily rimed crystals.

Hardness and density were measured eight times during the 81-hour observation period from 18 January to 21 January 2016. The hardness R of each snow layer was measured using a portable digital force gauge (AD-4932-50N) equipped with a circular plate with a diameter of 15 mm (Takeuchi et al., 1998). The vertical loads W of the snow over each snow layer were also measured.

To differentiate between each snow layer in the snow cover, red yarns were placed on new snow as a marker at time intervals of 3 to 24 hours when snow accumulated (Fig. 1a). Figure 1b shows a cross-section of a snow pit at the last observation at 12:00 Japan Standard Time (JST) on 21 January. Each red yarn indicates the boundary between two snow layers.

2.2 Calculation of compressive viscosity for each snow layer

To evaluate the stability of snowpack on a slope during snowfall, the compressive viscosity η must be known. The viscosity η is expressed in Equation (1) based on the viscous compression theory for snowpack (e.g., Kojima, 1975):

$$W_i = -\eta \frac{dh_i}{h_i dt} = \eta \frac{d\rho_i}{\rho_i dt} \ . \qquad (1)$$

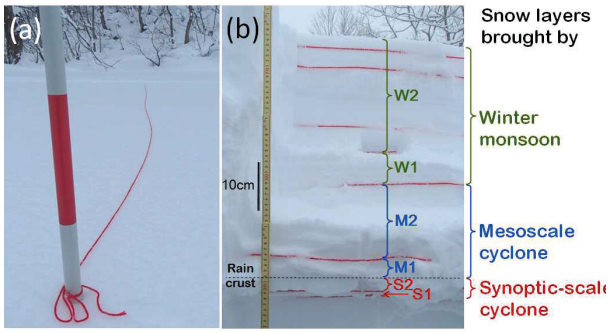

Figure 1: Field observations using red yarn: (a) red yarn placed on snow surface as a marker to differentiate between snow layers, (b) the cross-section of snow pit at the last observation at 12:00 Japan Standard Time (JST) on 21 January.

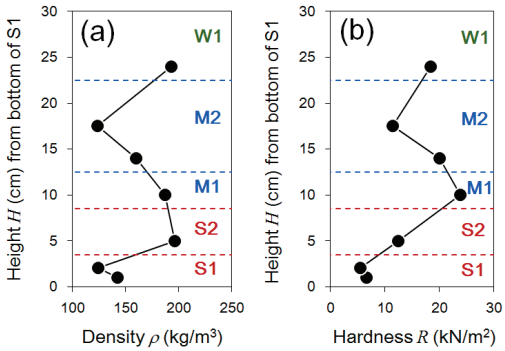

Figure 2: Vertical profiles of (a) density ρ and (b) hardness R of snow from S layer to the lower part of W layer observed at 12:00 JST on 21 January.

Where η is the compressive viscosity (N·s/m^2), h_i is thickness of layer i (m), ρ_i is the density of layer i (kg/m^3), W_i is the vertical load exerted by snow overlying layer i (N/m^2), t is the duration of loading on layer i (s). The viscosity η can be obtained by using Equation (2), which is a transformation into the differential form of Equation (1):

$$\eta(t) = \frac{\overline{W}(t) \cdot \Delta t \cdot \overline{\rho}(t)}{\rho(t+\Delta t) - \rho(t)} \quad , \tag{2}$$

where,

$$\overline{W}(t) = \left(W(t) + W(t+\Delta t)\right)/2 \quad , \tag{3}$$

$$\overline{\rho}(t) = \left(\rho(t) + \rho(t+\Delta t)\right)/2 \quad . \tag{4}$$

The viscosity η of each snow layer was calculated using Equations (2), (3), and (4) based on the measured density ρ of each layer and the measured vertical load W of snow over each layer. Then the compressive viscosities η in each snow layer were used to evaluate the stability of snowpack on the slope described in the next section.

2.3 Evaluating the stability of snowpack

One factor relating to avalanche occurrence is the stability of the snowpack on the slope. We used a classical stability index SI that expresses the ratio of shear strength to shear stress for the snowpack on the slope (Endo, 1993; Conway and Wilbour, 1999; Schweizer et al., 2003):

$$SI = \frac{\Sigma_s}{H\rho g \sin\psi \cos\psi} \quad , \tag{5}$$

where Σ_s is the shear strength of the snow layer (N/m^2), H is the depth of new snow above the snow layer (m), ρ is the density of new snow above the snow layer (kg/m^3), g is gravitational acceleration (m/s^2), ψ is the slope inclination (°), and $H\rho g \sin\psi \cos\psi$ is the shear stress acting on the snow layer (N/m^2). The vertical load W (N/m^2) imposed by snow above the snow layer is $H\rho g$.

The shear strength $\Sigma_s(t)$ of a snow layer at time t can be estimated using Equation (6) with respect to snow density $\rho(t)$ at time t (Endo, 1993):

$$\Sigma_s(t) = 3.10\times10^{-4}\,\rho(t)^{3.08} \quad . \tag{6}$$

However, the snow density ρ increases with time t during snow accumulation because of the densification of the snowpack (Refer to Equation (1)). Increased snow density $\rho(t)$ (kg/m^3) at time t was calculated by using viscous compression theory, shown in Equation (7) (Endo, 1993):

$$\rho(t) = \left\{ \frac{\beta I_w g}{2\alpha} \cdot \cos^2\psi \cdot t^2 + \rho_0^{\beta} \right\}^{1/\beta} \quad , \tag{7}$$

where ρ_0 is the initial density of the snow layer (kg/m^3) and I_w is the snowfall intensity (kg/m^2·s). The snowfall intensity I_w is related to the snowfall intensity I_h (m/s) obtained from the change in observed snow depth at the time intervals of observation such that $I_w = \rho_0 I_h$. The increased snow density $\rho(t)$ was used to estimate the shear strength Σ_s of the snow layer shown in Equation (6). α (N/(m^2·s·(kg/m^3)$^{\beta}$)) and β in Equation (7) are coefficients related to the densification of the snowpack and can be obtained from Equation (8), with respect to snow density $\rho(t)$ (kg/m^3) and compressive viscosity $\eta(t)$ observed in the field measurement:

$$\eta(t) = \alpha\rho(t)^{\beta} \, . \tag{8}$$

Using Equations (5), (6), (7), and (8), we can calculate the temporal variation in the stability index SI for snow layers consisting of unrimed and heavily rimed crystals based on the result of field observation.

3. RESULTS OF FIELD OBSERVATION

3.1 *Overview of snow cover during the period of field observation*

Figure 1b shows a cross-section of a snow pit at the last observation at 12:00 JST on 21 January. The thickness of each layer in the last observation is 8.5 cm for the S layer (S1 and S2), 14 cm for the M layer (M1 and M2), and 44 cm for the W layer (W1 and W2).

Figure 2 shows vertical profiles of density and hardness of snow from S1 to the lower part of W1 at the last observation. The density and hardness of the lower part of the S layer (S1), which is at the bottom of the snow that accumulated during the period of field observation, has the lowest values of any snow cover. Therefore, the S layer will acts as the weak layer with related to the stability of snowpack on the slope.

3.2 *Characteristics of snow crystals*

Figure 3 shows photographs of snow crystals from the S1 layer. The S1 layer (hereinafter, referred to as "S layer") was composed of transparent unrimed crystals and lightly rimed crystals. These were hexagonal plates, dendrites with broad branches, and spatial plates. These snow crystals formed in the stratiform clouds of the synoptic-scale cyclone. The crystals maintained their shape during the period of field observation.

Figures 4 shows photographs of snow crystals from the M1 and M2 layers (hereinafter, referred to as "M layer"). For the M layer, many frozen cloud droplets were attached to the crystals and were not transparent. Therefore, the M layer contained many heavily rimed crystals and graupels. These crystals formed in convective clouds that are associated with mesoscale cyclone.

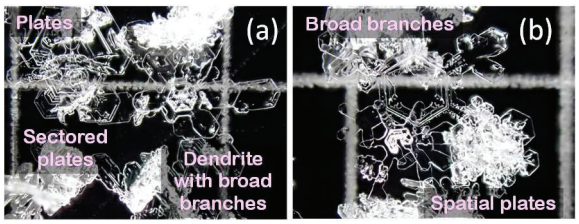

Figure 3: Snow crystals in S1 layer observed at 03:00 JST on 18 January. Mesh in background has intervals of 3 mm. (Photo: Shinji Ikeda)

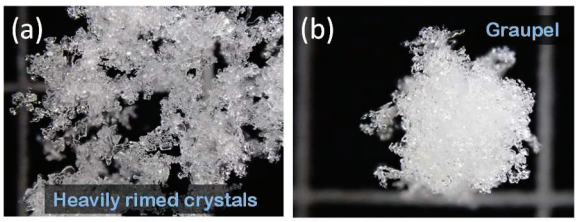

Figure 4: Snow crystals in (a) M1 layer observed at 18:00 JST on 19 January and (b) M2 layer observed at 06:00 JST on 20 January. Mesh has intervals of 3 mm. (Photo: Shinji Ikeda)

To understand the difference in temporal changes in the densities and hardnesses of snow layers consisting of unrimed versus heavily rimed crystals, we addressed the S layer as the non-persistent weak layer consisting of unrimed crystals and the M layer as snow consisting of heavily rimed crystals.

3.3 *Temporal changes in snow density and hardness*

Figure 5 shows the temporal changes in densities and hardnesses of the S layer and the M layer. The solid lines in Fig. 5 are regression lines of the densities and hardnesses for time elapsed from the first observations for each layer. The density and hardness increased more slowly in the S layer, which consisted of unrimed crystals, than in the M layer. The rates of increase in the density and hardness of the S layer were 35% and 12% those of the M layer, respectively.

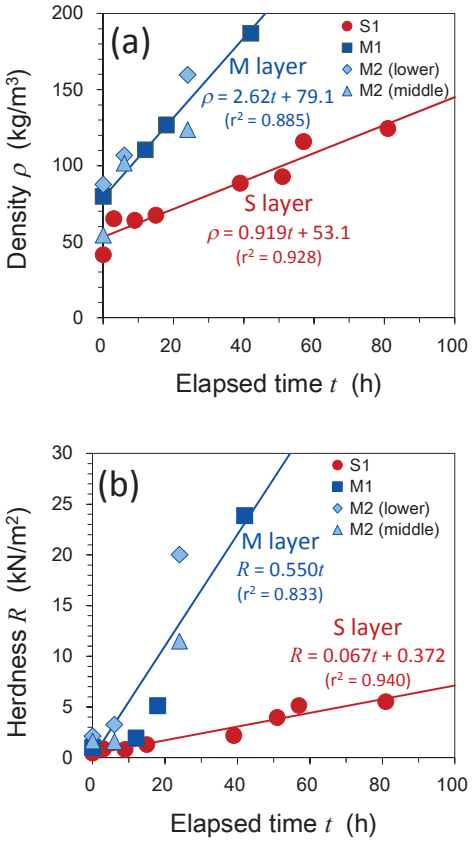

Figure 5: Temporal changes in (a) densities ρ and (b) hardnesses R for S layer and M layer. The time on horizontal axis is time elapsed from the first observation for each layer. Solid lines are regression lines, r^2 are coefficients of determination.

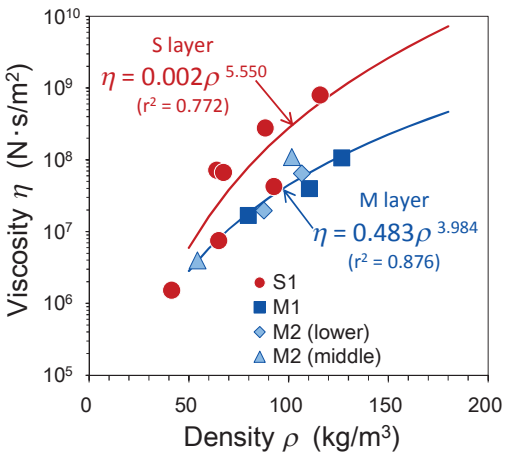

Figure 6: Relationship between density ρ and compressive viscosity η of S layer and M layer.

The S layer was composed of unrimed dendrites with broad branches and unrimed spatial plates (Fig. 3). These crystals are less prone to compress than are other crystals, such as stellar crystals and dendrites with narrow branches (Goto et al., 2005). Therefore, the density ρ of the S layer will remain low. On the other hand, bonding between snow crystals in the M layer will grow because of sintering between crystals to which many cloud droplets are attached, so the hardness R of the M layer tends to increase rapidly.

3.4 Compressive viscosity

Figure 6 shows the relationship between the compressive viscosity η and the density ρ of the S layer and the M layer. The viscosity η of the S layer, which consists of unrimed crystals, is higher than that of the M layer, which consists of heavily rimed crystals. The high value of viscosity η means that the strain rate is low and the density ρ increases slowly for a given vertical load W (Refer to Equation (1)).

Regression analysis between the viscosity η and the density ρ in Fig. 6 gives the coefficients α and β in Equations (7) and (8): For the S layer, α = 0.002 and β = 5.55 (r^2 = 0.772, number of data n = 7); for the M layer, α = 0.483 and β = 3.98 (r^2 = 0.876, n = 7).

4. RESULTS OF A THEORETICAL EXAMINATION ON STABILITY OF SNOWPACK

4.1 Estimating the stability of snowpack

The stability indices SI for the S layer and the M layer will be examined by using the coefficients α and β obtained from the field observation (Fig.6). In calculating the stability indices SI, the initial densities ρ_0 of the S layer and the M layer were 50 kg/m³ and 80 kg/m³, respectively, because these values approximate the observed newly fallen snow densities (Fig. 5a). We assumed that snow continued to accumulate with constant snowfall intensity I_h on slope with an inclination ψ of 45°, and we calculated the stability indices SI for the S layer consisting of unrimed crystals and for the M layer consisting of heavily rimed crystals.

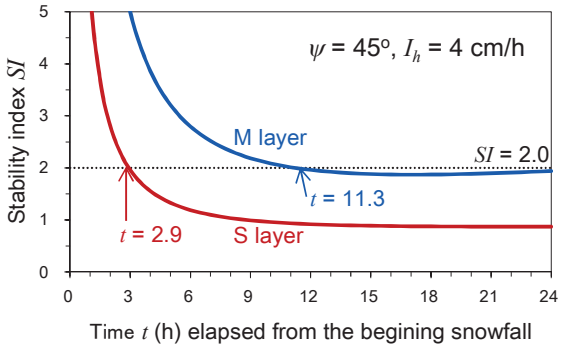

Figure 7: Example of temporal variations in the stability indices SI for S layer and M layer estimated for the conditions of constant snowfall intensity I_h of 4 cm/h and slopes inclination ψ of 45°.

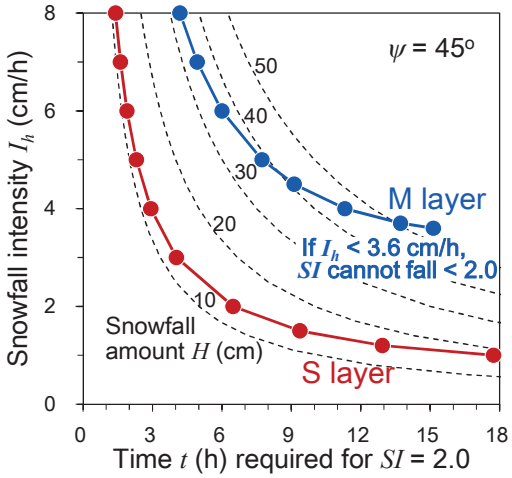

Figure 8: Relationship between the time t required for the stability index SI to fall to 2.0 from the beginning of snowfall and the snowfall intensity I_h on slope with inclination ψ of 45°.

Figure 7 shows an example of estimated temporal variations in the stability indices SI for the S layer and the M layer. According to Nishimura et al. (2006), the frequency of avalanches increases remarkably when the stability index SI falls below 2.0. In Fig. 7, we also assumed that avalanches are likely to occur when the stability index SI is below 2.0. Figure 7 indicates that the time t required for the stability index SI of the S layer to fall to 2.0 is shorter than that of the M layer.

4.2 *Evaluating the failure of non-persistent weak layer during snowfall*

Figure 8 indicates the relationship between the snowfall intensity I_h and the time t required for the stability index SI to fall below 2.0 after snowfall began. When the snowfall intensity I_h is 8 cm/h (i.e., extreme heavy snowfall), for the M layer, the stability index SI falls to 2.0 at about 5 hours after snowfall begins. The snowfall amount during that time is over 30 cm. It is a condition of snowfall amount under which avalanche release are common (e.g., Schweizer et al., 2003). Moreover, for the M layer, the time t required for the stability index SI to fall below 2.0 and snowfall amount during that time increases with decreases in snowfall intensity I_h. However, if the snowfall intensity I_h is less than 3.6 cm/h on a slope with an inclination of 45°, then the stability index SI cannot fall below 2.0, and the avalanche likelihood will be low.

For the S layer, the stability index SI tends to fall below 2.0 more rapidly with less snowfall amount than for the M layer. If the snowfall intensity I_h exceeds 4 cm/h (i.e., heavy snowfall), then the stability index SI for the S layer becomes 2.0 within a few hours of the snowfall amount reaching about 15 cm. In addition, even when the snowfall intensity I_h is below 2 cm/h (i.e., usual snowfall), the stability index SI of the S layer can fall below 2.0.

5. CONCLUSIONS

Snow consisting unrimed crystals (i.e., the non-persistent weak layer), such as in the S layer, undergoes rapid destabilization at less snowfall than the snow consisting of heavily rimed crystals, such as in the M layer. Therefore, when snow such as that in the S layer accumulates, an early warning of avalanche occurrence is required, even when little snow has fallen.

This paper proposed a method for evaluating the likelihood of avalanche releases triggered by the non-persistent weak layer using the snowfall intensity and the time required for the stability index to fall to 2.0. However, heavy snowfall of unrimed crystals such as that which occurs in Japan is rare here. We should accumulate cases in order to verify the evaluation shown in this paper.

ACKNOWLEDGEMENTS

The field observations were planned and carried out by Hiroki Matsushita, who is one of the authors, and the late Shinji Ikeda. We particularly thank Dr. Ikeda for his great collaboration. We also thank Shigeru Ishikawa of the Snow Avalanche and Landslide Research Center, PWRI for his support in the field observations.

REFERENCES

Akitaya, E. and H. Shimizu, 1987: Observations of weak layers in a snow cover. Low Temperature Science, A46, 67-75. (In Japanese with English abstract)

Bair, E. H., 2011: Fracture mechanical and statistical properties of avalanches that fail on nonpersistent snow crystals. Ph. D. Thesis, University of California, 183 pp.

Bakkehøi, S., 1986: Snow avalanche prediction using a probabilistic method. International Association of Hydrological Sciences (IAHS) Publications, 162, 549-555.

Brown, C. and B. Jamieson, 2006: Evolving shear strength, stability and snowpack properties in storm snow. Proceedings of the International Snow Science Workshop, Telluride, CO, 15-21.

Brown, C. and B. Jamieson, 2008: Shear strength and snowpack stability trends in non-persistent weak layers. Proceedings of the International Snow Science Workshop, Whistler, BC, 939-947.

Conway, H. and C. Wilbour, 1999: Evaluation of snow slope stability during storms. Cold Regions Science and Technology, 30, 67-77.

Endo, Y., 1993: Forecasting of direct-action avalanches in terms of snow accumulation rates. Seppyo (Journal of the Japanese Society of Snow and Ice), 55, 113-120. (In Japanese)

Gauthier, D., C. Brown, and B. Jamieson, 2010: Modeling strength and stability in storm snow for slab avalanche forecasting. Cold Regions Science and Technology, 62, 107-118.

Goto, H., M. Kajikawa, M. Hashimoto, N. Goto, and K. Kikuchi, 2005: Relationship between compressive viscosity of dry new snow and characteristics of snow particles. Seppyo (Journal of the Japanese Society of Snow and Ice), 67, 331-340. (In Japanese with English abstract)

Hirashima, H., K. Nishimura, S. Yamaguchi, A. Sato, and M. Lehning, 2008: Avalanche forecasting in a heavy snowfall area using the snowpack model. Cold Regions Science and Technology, 51, 191-203.

Ikeda, S., 2015: Formation and persistence of snow instability associated with precipitation-induced weak layer that caused Mumeizawa avalanche accident. Seppyo (Journal of the Japanese Society of Snow and Ice), 77, 17-35. (In Japanese with English abstract)

Kojima, K., 1975: A field experiment on the rate of densification of natural snow layers under low stresses. Proceedings of the Grindelwald Symposium, IAHS Publication, 114, 298-308.

Matsushita, H. and K. Ishida, 2016: Characteristics of snow avalanche release in forests during a heavy snowfall event. Proceedings of the International Snow Science Workshop, Breckinridge, CO, 556-560.

McClung, D. M. and P. A. Schaerer, 2006: The Avalanche Handbook. The Mountaineers, 347 pp.

Nishimura, K., H. Hirashima, M. Lehning, K. Ishimoto, and H. Kawami, 2006: Development of snow avalanche danger index II. Proceedings of Cold Region Technology Conference, 22, 31-35. (In Japanese)

Schweizer, J., J. B. Jamieson, and M. Schneebeli, 2003: Snow avalanche formation. Reviews of Geophysics, 41, 1016, doi: 10.1029/2002RG000123.

Takeuchi, Y., Y. Nohguchi, K. Kawashima, and K. Izumi, 1998: Measurement of snow-hardness distribution. Annals of Glaciology, 26, 27-30.